COMPDYN 2013
4th ECCOMAS Thematic Conference on
Computational Methods in Structural Dynamics and Earthquake Engineering
M. Papadrakakis, V. Papadopoulos, V. Plevris (eds.)
Kos Island, Greece, 12–14 June 2013

VISK: A GIS-COMPATIBLE PLATFORM FOR MICRO-SCALE ASSESSMENT OF FLOODING RISK IN URBAN AREAS

R. De Risi[1], F. Jalayer*[1,2], I. Iervolino[1,2], G. Manfredi[1,2], and S. Carozza[1]

[1] Università degli studi di Napoli Federico II, Naples, Italy.

[2] Analisi e Monitoraggio dei Rischi Ambientali s.c.ar.l., Naples, Italy.

*Corresponding author

e-mail: {raffaele.derisi, fatemeh.jalayer, iunio.iervolino, gaetano.manfredi} @unina.it

Keywords: Fragility, vulnerability assessment, portfolio of structures, Bayesian parameter estimation, Graphical user interface.

Abstract. *Evaluation of the vulnerability of buildings in urban areas to flooding is a fundamental step in flooding risk mitigation. In this work, a new GIS-compatible computer platform with Matlab®-based graphical user interface is presented: VISK, "Visual Vulnerability & Risk", flooding module. This platform performs detailed (micro-scale) flood risk assessment for building stock with more-or-less similar characteristics. The GIS compatibility allows for graphical processing of both input and output to the program, providing an efficient visualization of flooding risk. At the core of the platform lies a comprehensive probability-based algorithm for the assessment of the vulnerability of a class of buildings to flooding. This Bayesian algorithm is based on assigning prescribed analytic uni- and bi-modal probability distributions for characterizing the flooding structural fragility functions. This allows for efficient evaluation of structural fragility based on a small number of (around 30-50) Monte Carlo simulations. The fragility calculations are performed on a bi-dimensional finite-element structural model considering the openings (door and windows) constructed using open-source software Opensees. The uncertain structural modeling parameters are characterized through, orthophoto recognition, sample in-situ building survey, laboratory test results for material mechanical properties and literature survey. Finally, the risk map is generated by integrating the flooding hazard and fragility taking into account additional information on the exposure (e.g., repair costs, population density, etc.). The results can be visualized both in a detailed building-to-building scale (of potential interest to single house-holds) or as overall estimates for the entire area (of interest to policy makers).*

1 INTRODUCTION

Delineation of flood prone areas and the evaluation of the vulnerability of buildings in the urban areas to flooding are fundamental steps in taking adaptive measures for flooding risk. This demands cross-cutting scientific and technical support from different disciplines, such as but not limited to, climate modeling, hydraulic engineering, structural engineering, risk modeling and urban policy making. In recent years, increasing attention is focused on flooding risk assessment. In fact, several publications document and discuss the consequences of flooding, such as loss of life [1], economic losses [2-4] and damage to buildings [5-8]. These research efforts have many aspects in common, such as a direct link between the flooding intensity and the incurred damage, and that they are based on real damage observed in the aftermath of a flooding event. On the other hand, many research efforts are starting to galvanize in the direction of proposing analytical models for flood hazard and vulnerability assessment taking into account various sources of uncertainties. For instance, in [9] a stochastic method for assessment of the direct impact of flood actions on buildings is proposed. A general methodological approach to flood risk assessment is embedded in the HAZUS procedures for risk assessment [10, 11]. Moreover, [12] provides a classification of flood risk assessment methods based on their degree of complexity and precision. In this context, development of tools that allow for quantifying flooding risk efficiently and with sufficient accuracy is essential. These methods serve as technical support to the stakeholders and policy makers, for flood risk mitigation, emergency preparedness, response and recovery, both in short- and long-term.

In this work, a new software tool for flood risk assessment for individual buildings is presented. VISK, acronym of Visual Vulnerability and (*Flooding*) Risk, is a GIS-compatible platform that performs micro-scale flood risk assessment for buildings located in homogenous (i.e., characterized as a single *class* of buildings) urban areas. Figure below demonstrates the graphical user interface for VISK.

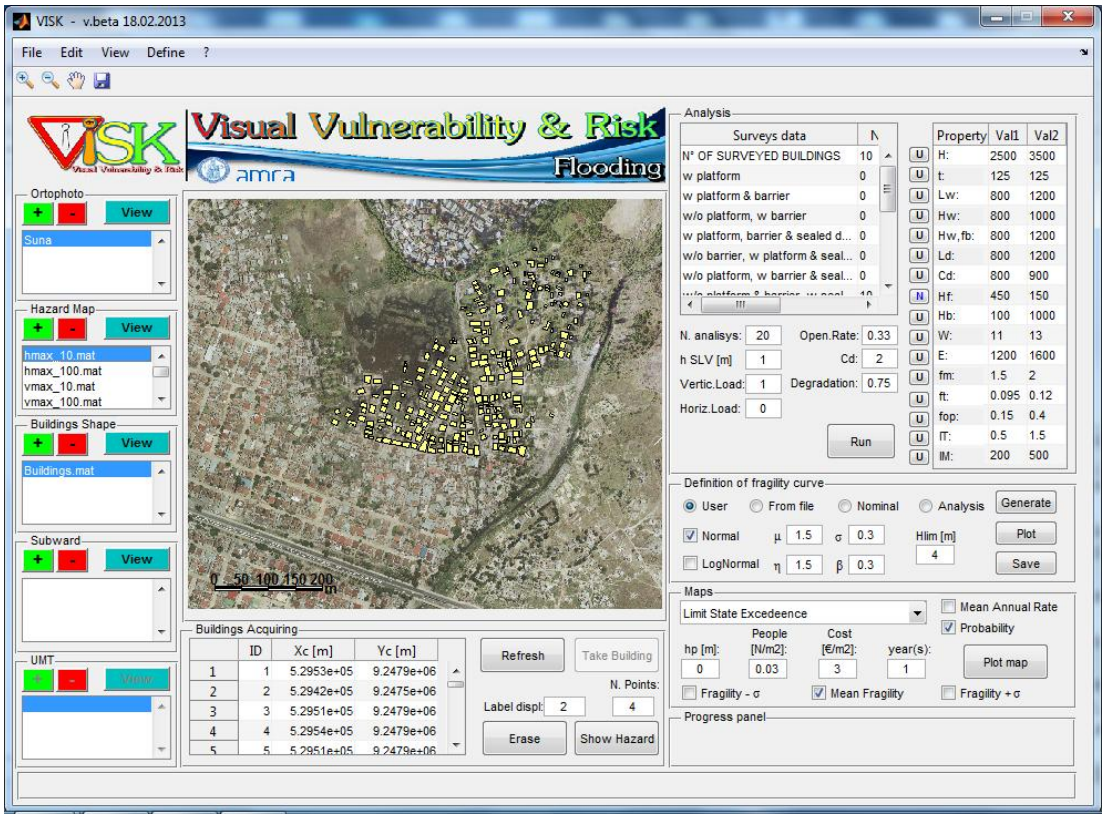

Figure 1: The graphical user interface for VISK.

The main parts of the graphical user interface for VISK are: (1) the central display panel in which the orthophoto of the case study area is demonstrated. The orthophoto can be overlaid on the spatial polygons representing buildings' foot-prints (i.e., a GIS shape file) and the flooding height/velocity profile for a prescribed return period; (2) the orthophoto input panel where an orthophoto of the case-study area can be up-loaded; (3) the flood profile panel where a lattice of nodes containing maximum flood depth and velocity pairs for each node for a given return period can be up-loaded; (4) building shape panel where the GIS shape file of the buildings' spatial boundary can be up-loaded; (5) a panel for miscellaneous information in which data such as spatial delineation of administrative boundaries can be up-loaded; (6) a panel for the acquisition of data regarding buildings' spatial foot-prints, where in lieu of shape files, for each building, the spatial foot-print can be specified manually and processed by the program; (6) a digital survey sheet where the results of building-specific field survey can be specified. This digital panel is matched with a building-specific survey sheet; (7) a structural analysis panel where a specified number of structural model realizations are generated and analyzed based on the data provided by the digital survey sheet; (8) a fragility assessment panel where the fragility curves for a specified limit state are derived based on the results of the simulations performed in the structural analysis panel. This panel also envisions up-loading of user-defined fragility curves; (9) risk map generation panel where risk maps are plotted for various risk metrics such as the frequency of exceeding a given limit state, expected repair/replacement costs, etc; (10) a progress panel which visualizes the progress of the program. In the following, various functionalities of VISK are discussed in detail. In order to render the description more accessible, each section is accompanied by a numerical example.

Background: VISK is created inside the European FP7 project CLUVA**:** Climate change and urban vulnerability in Africa. The original idea was to create a tool for vulnerability assessment of informal settlements in Africa. The problem of vulnerability assessment for a portfolio of "informal" and non-engineered buildings is particularly challenging due to many aspects such as lack of complete information and poor construction details. In fact, the core vulnerability assessment methodology created for VISK is organized in a manner so that various sources of uncertainty can be taken into account, with particular attention to structural detailing and water-tightness. Moreover, due to lack of precise survey data, the software uses sample surveys as a basis and constructs probability distributions for the probability of observing/not observing certain structural details in a given building in a Bayesian framework. Needless to say, VISK as a visual interface and platform for vulnerability and risk assessment is applicable not only to the non-engineered structures in an African context but also to other structural typologies in alternative contexts.

2 INPUT DATA

The input data required by platform VISK are: orthophoto of the case-study area, spatial foot-print of the buildings, flooding height/velocity profiles for prescribed return periods and the uncertainties in structural modeling parameters related to both material mechanical properties, construction details and geometry (in the form of probability distributions). In this section, each input category is described in more detail.

2.1 Othophoto and the footprint of the buildings

The orthophoto of the case-study area needs to have the following characteristics: at least 300 dpi of resolution, aspect ratio of about one, georeferenced in a specific coordinate system (e.g., UTM,WGS 1984) that remains the same for all the other input (i.e. flood hazard maps, buildings shape). As far as it regards the spatial foot-print of the buildings to be analyzed, the

program accepts a dataset containing the information stored for each spatial polygon that defines the building boundary (i.e., a GIS shape file format). In case such a spatial dataset is not available, VISK can extract the plan dimensions by performing orthophoto boundary recognition guided by the user. User's role is to manually define the nodes of the polygon that define building's footprint as illustrated in Figure 2 below. The user-guided boundary recognition operation not only helps in creating a digital database of buildings for which risk assessment is later going to be performed but also helps in characterizing the building-to-building variability in the dimension of the wall which is going to resist the flood action.[1]

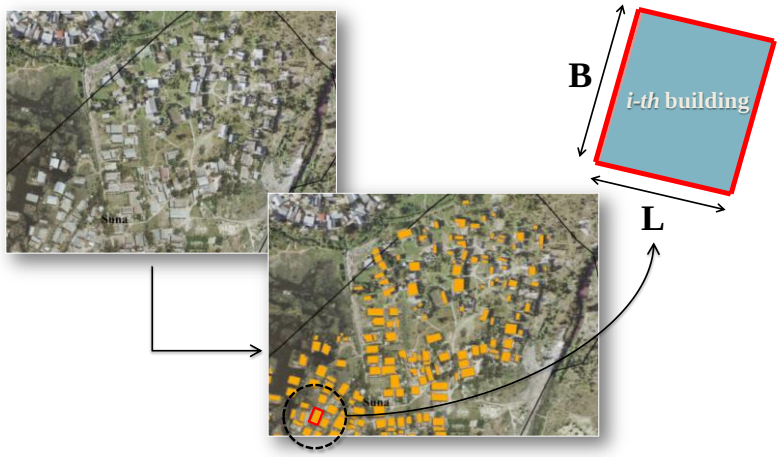

Figure 2: Acquisition of data regarding building footprint.

2.2 Characterization of uncertainties:

VISK can be used for flooding risk assessment for individual buildings located in a homogenous urban area. Therefore, the main function of VISK as software for vulnerability assessment is the definition of fragility curves for a single class of structures. Therefore, the uncertainties considered are primarily related to building-to-building variability in material properties, geometry and construction details. In the following sub-sections, the procedure for characterizing these uncertainties is described in detail. As mentioned in the previous section, orthophoto recognition can be used in order to capture the variation of buildings' footprints in the case-study area. However, building specific field surveys are needed in order to gain better understanding of the geometry and construction details. As far as it regards survey-based input requirements for VISK, information on the uncertain parameters can be specified in two alternative ways: (1) discrete binary uncertain parameters based on a logic-tree approach; (2) continuous uncertain parameters.

2.2.1 Discrete binary uncertain parameters/logic statements:

Presence of raise-foundation / Platform	*PL*
Presence of Barrier	*Ba*
Are the doors sufficiently water-proof	*DS*
Are the windows sufficiently water-proof	*WS*

[1] Neglecting the effect of internal walls or embedded columns in reducing the "free" loading span.

Is There a door in the wall panel	*D*
Are there windows in the wall panel	*W*
Are there signs of material degradation	*DG*

Table 1 - Discrete binary uncertain parameters considered by VISK

Table 1 reports the list of discrete binary uncertain parameters/logic statements considered and the related input accepted by VISK. Examples of the uncertain binary parameters considered are, presence of a raised foundation (platform) *Pl*, presence of a barrier *Ba*, water-tightness of the door *DS*, water-tightness of the windows *WS*, and presence of a visual degradation in the building *DG*. It can be noted that also the presence of openings (doors *D* and windows *W*) in the model wall panel is randomized. This is due to fact that in the current version of VISK, the specific building wall hit first by the flood (and its angle) are assumed to be unknown. The vulnerability assessment module uses the logic-tree approach in order to propagate the uncertainties in discrete binary uncertain parameters listed in Table 1. Organization of the binary parameters in a logic-tree, among other things, enables the user to define the correlation between various uncertain parameters. Figure 3 below illustrates the two logic-trees employed by VISK: (a) the logic tree illustrated in Figure 3a is used in order to evaluate whether the building is sufficiently waterproof or not; (b) the logic-tree illustrated in Figure 3b is used in order to randomize the wall panels in terms of the presence of openings (door and windows). The red arrows indicate the information that should be input to VISK.

n° OF SURVEYED BUILDINGS	100
n° of buildings with visual signs of degradation DG	0
n° of buildings with ***Pl***	30
n° of buildings with ***Ba given Pl***	10
n° of buildings with ***Ba given not Pl***	50
n° of buildings with DS given ***Pl*** and ***Ba***	5
n° of buildings with DS given ***Pl*** and not ***Ba***	15
n° of buildings with DS given not ***Pl*** and ***Ba***	30
n° of buildings with DS given not ***Pl***, not ***Ba***	8
n° of buildings with WS given ***Pl***, ***Ba***, and ***DS***	2
n° of buildings with WS given ***Pl***, not ***Ba***, and ***DS***	5
n° of buildings with WS given not ***Pl***, ***Ba***, and ***DS***	10
n° of buildings with WS given not ***Pl***, not ***Ba***, and ***DS***	3
n° OF SURVEYED WALLS	400
n° of walls with ***D***	100
n° of walls with W given ***D***	80
n° of walls with W given not ***D***	200

Table 2 - Example: Discrete binary uncertain parameters in a sample survey data input to VISK.

Logic-trees: Logic-tree [13] is an efficient and visual method for modeling the joint probability distribution for several discrete uncertain variables represented as logic statements. A logic tree is consisted of *nodes*, *branches* and *paths*. Each node represents a logic statement (e.g., given value of an uncertain parameter). Each branch in a logic-tree represents the degree of belief (conditional probability) for the logic statement in the destination node given all the statements corresponding to the nodes along the path leading to (and including) the node in the origin of the branch. For example, In Figure 3(a),(b), the degrees of belief or the condi-

tional probability values are written in grey characters on the corresponding branch **(**|, reads as *given* or *conditional on***)**. Each path in a logic-tree is consisted of nodes and branches that connect them; where the nodes belong to progressively increasing levels within the tree. The degree of belief in a path (or the joint probability for the specific values of the corresponding uncertain parameters) is equal to the product of the probabilistic corresponding to the branches that construct the path. Finally, for any vertical cut to the tree, the sum of the degrees of belief for all the paths trimmed by the cut should be equal to unity. That is, the paths trimmed by vertical cuts represent mutually exclusive and collectively exhaustive logic statements.

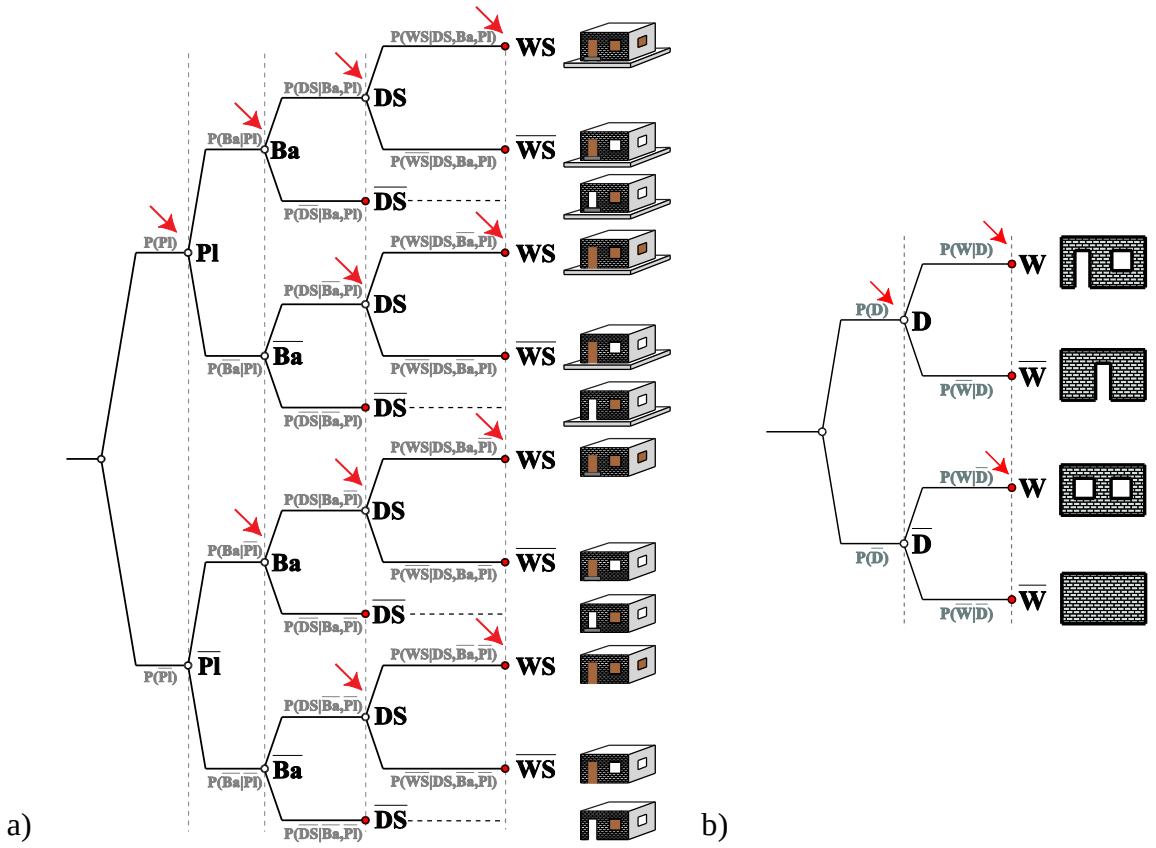

Figure 3: a) logic tree for the waterproofness, b) logic tree for the modeling generation.

Estimating the logic-tree probabilities/degrees of belief: VISK's operative way to assess the conditional probability/degree of belief for each node of the logic tree, consists in cataloging of the survey information, following the conditions imposed by path leading to the node in question. The conditional probabilities corresponding to each branch can be constructed by classifying progressively the building survey results based on the logical value (truth value) of each binary statement. In fact, the visual survey panel in the graphical interface allows the user to progressively input the survey results based on the specific conditions imposed by the path. This provides the possibility to take into account the correlation between uncertain parameters/logic statements. It can be observed from Table 2 that the input data accepted by VISK for a binary uncertain parameter/logic statement denoted as BV is in the form of the number r of surveyed buildings (progressively classified as described above) for which the logic statement is TRUE out of number n of all the buildings surveyed. Therefore, the probability π that BV is true can be calculated as a complete Beta-function [14]:

$$p(\pi \mid r,n) = \frac{(n+1)!}{r!(n-r)!}\pi^{r}(1-\pi)^{n-r} \quad (1)$$

where $p(\pi|r,n)$ denotes the probability distribution for the degree of belief in statement BV given r "success" out of a total of n. After evaluating the above probability distribution, VISK platform provides three possibilities as much as it regards the estimation of π: a) only use the mode of the distribution in Eq. 1: $\pi = r/n$ b) only use the expected value $\pi = (r+1)/(n+2)$, that is the first moment approximation, or c) sample from the entire distribution.

Numerical example: With reference to the survey information reported in Table 2, using the mode of the Beta distribution in Eq. 1, referred to as approach (a) above: $P(Ba|Pl)$ is equal to 10/30=0.33; $P(DS|Ba,Pl)$ is equal to 5/10=0.5; and finally $P(WS|DS,Ba,Pl)$ is equal to 2/5=0.40.

2.2.2 Continuous uncertain parameters:

The VISK input for continuous uncertain parameters consists of the choice of a probability distribution (e.g., Normal or Uniform) and its relevant statistics. In the current version of VISK possible correlations between the continuous uncertain parameters are not considered. However, the future updates will allow for modeling of possible correlations between a chosen subset of the continuous parameters. These user-specified probability distributions will be used later during the simulation process.

Table 3, 4 and 5 list the continuous uncertain parametersparameter considered in VISK. It can be observed that the continuous parameters considered are classified into three categories: (1) parameters related to the building geometry; (2) parameters related to the mechanical material properties; (3) parameter related to structural loading.

Geometrical property	Distribution type	Mean Min	Standard Deviation Max
L (m) - wall length	Normal	11.17	3.39
H (m) - wall height	Uniform	2.50	3.50
t (m) - wall thickness	Deterministic	0.125	0.00
L_w (m) - window length	Uniform	0.80	1.20
H_w (m) - window height	Uniform	0.80	1.00
H_{wfb} (m) - window rise	Uniform	0.80	1.20
L_d (m) - door length	Uniform	0.80	1.20
C_d (m) - corner length	Uniform	0.80	0.90
H_f (m) - foundation rise	Lognormal	0.45	0.15
H_b (m) - barrier height	Uniform	0.10	1.00

Table 3: The continuous uncertain parameters considered by VISK: building geometry.

In the first category, parameters such as structural height, wall thickness, window length and height, window height from the bottom, door length, distance between the corners and the openings, the foundation (platform) height. As far as it regards the second category, parameters such as elastic modulus (E), Poisson ratio (ν), compressive strength (f_m), shear strength(τ_0), flexural strength (f_{fl}) for the wall panels are considered. Moreover, it possible to take into account a parameter that measures the amount of material deterioration due to the elongated contact with water.

Mechanical properties	Distribution type	Mean Min	Standard Deviation Max
f_m (MPa) - compression strength	Uniform	1.50	2.00
τ_0 (MPa) - shear strength	Uniform	0.095	0.12
f_{fl} (MPa) - flexural strength	Uniform	0.14	0.40
E (MPa) - linear elastic modulus	Uniform	1200	1600
G (MPa) - shear elastic modulus	Uniform	500	667
γ (kN/m^3) - self weight	Uniform	11	13

Table 4: The continuous uncertain parameters considered by VISK: material mechanical properties.

Ideally, input statistics related to structural material properties should be obtained based on the results of case-specific laboratory tests. The laboratory tests are aimed to mimic the construction materials and relevant techniques used in the field, in order to evaluate the main mechanical characteristics of the wall material. In lieu of case-specific laboratory tests, existing literature results can be used. Third category is related to uncertain loading parameters. Table 5 report the uncertain parameters *a* and *b* related to the hydro-dynamic flood loading profile. These parameters describe the flooding velocity as a power-law function ($a \cdot h^b$) of flooding height at a given point.

Loading parameter	Distribution type	Median	Standard Deviation
B	Lognormal	1.57	0.54
A	Fully correlated with b[2]		

Table 5: The continuous uncertain parameters considered by VISK: loading parameters

Numerical example: The histogram in Figure 4 illustrates the histogram of platform heights based on the results of sample field survey. A Lognormal distribution is fit to the histogram and its two parameters (median and logarithmic standard deviation) can be provided as input to VISK.

[2] b is sampled from a probability distribution fit to various (a, b) data pairs calculated based on the inundation profile. Therefore, after simulating b from its probability distribution, the closest (a, b) pair is taken.

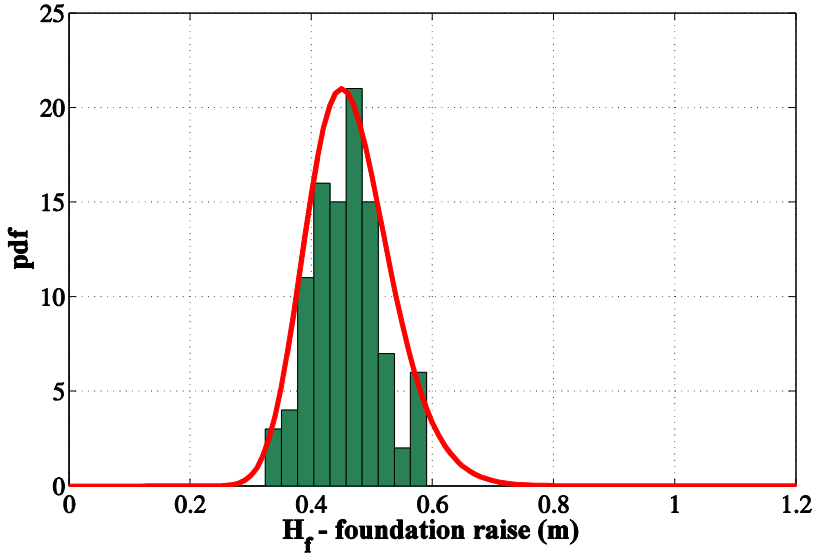

Figure 4: Histogram of platform height [17].

2.3 Hydraulic results and flooding hazard curves

Inundation profiles calculated for various return periods are one of the main input data fed into VISK. The inundation profile is generally expressed in terms of flood depth and velocity, for different return periods of the extreme precipitation event, for each node within a lattice that covers the entire case study area. This information is usually obtained through a general hydrologic/hydraulic routine. VISK acquires inundation profiles for various return periods, in terms of gridded data set in Arc ASCII grid format, typical output file of commercial software that develop mono/bi-dimensional diffusion models [15, 16].

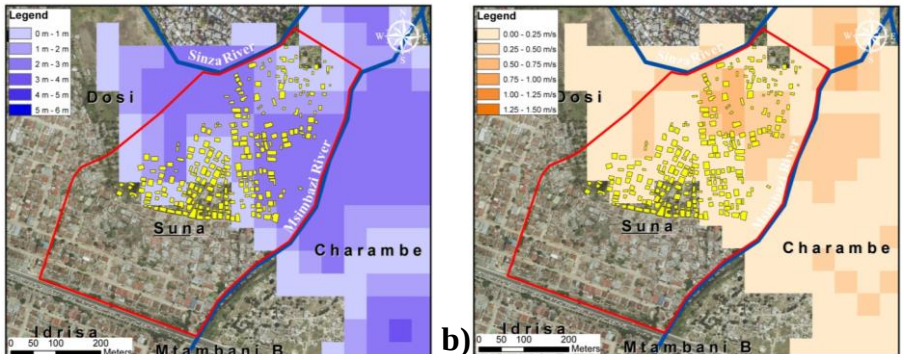

Figure 5: Inundation profiles for a given return period in terms of a) flood depth and b) flood velocity [17].

Once the grid dataset of the inundation profiles has been acquired by VISK, the software creates an overlay of the inundation profile (for various return periods and classified by flooding height and/or velocity) and the uploaded orthophoto of the case-study area.

Extracting flooding hazard curves: VISK has the capability of extracting flooding hazard curves in terms of the mean annual frequency of exceeding (equal to the inverse of return period for a homogenous Poisson process) a given flooding height or velocity for a given point within the case-study area (e.g., centroid of a given building), based on the input grid data set described in the previous paragraph. This is done by a spatial interpolation between the point

(identified as *G* in Figure 6 below) and the flood height/velocity values at the vertex of the lattice grid containing the point in question.

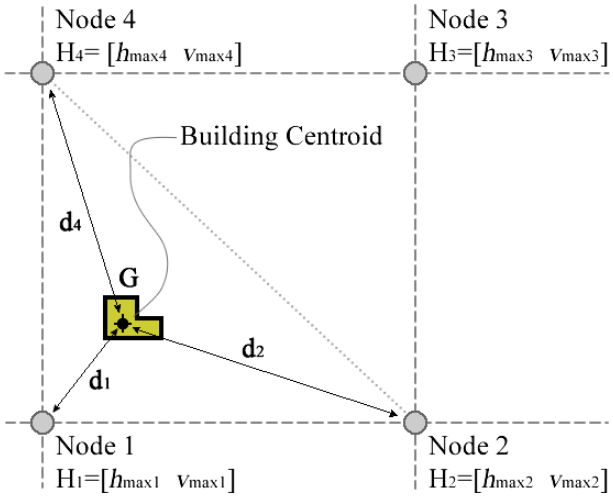

Figure 6: Graphical representation of the spatial interpolation for point G.

The flooding height and velocity vector denoted by $\mathbf{H}=[h_{max}, v_{max}]$ at a given point can be evaluated as follows:

$$H_G = \frac{\frac{H_1}{d_1} + \frac{H_2}{d_2} + \frac{H_4}{d_4}}{\frac{1}{d_1} + \frac{1}{d_2} + \frac{1}{d_4}} \tag{2}$$

where d_i denotes the distance to node i and H_i represents the flooding height and velocity vector for node i. It can be observed in Eq. 2, that the flood height and velocity vector H_G is calculated as the spatial weighted average of H_i; where the weights are equal to the inverse of the distance d_i. It is worth noting that for each building only the three closest nodes are considered.

Velocity/height relationship: For each point/centroid of a building, An analytic power-law relation of the form of $h_{max}=a\ v_{max}^{\ b}$ is fitted by employing a linear regression in logarithmic scale to $\mathbf{H}=[h_{max}, v_{max}]$ pairs for all the return periods considered. Figure 7 below demonstrates 3 different power-law fits for three different points within a case-study area. This power-law fit helps in transforming an otherwise vector-based risk assessment using $\mathbf{H}=[h_{max}, v_{max}]$ as the hazard/fragility interface variable to a scalar risk assessment problem using only h_{max} as the interface variable.

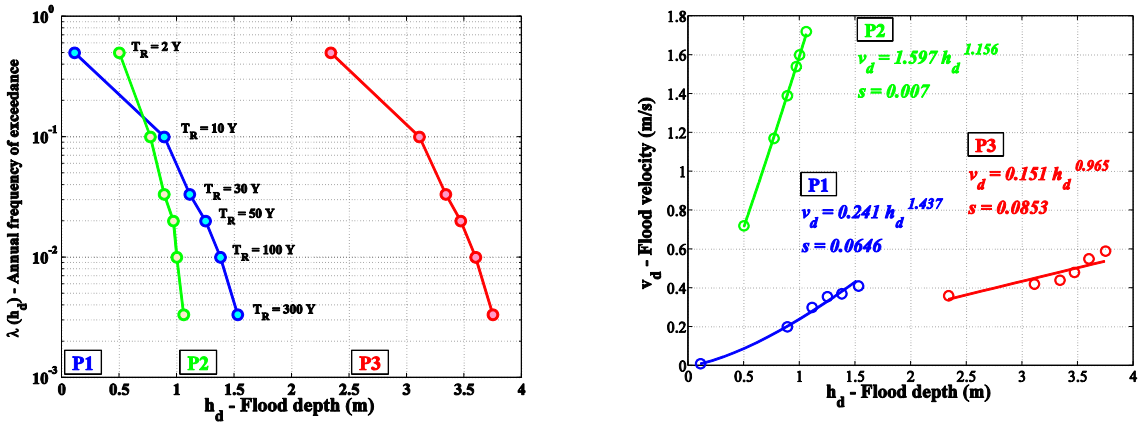

Figure 7: (a) Hazard curves, (b) Flood height versus flood velocity power-law relation [18]

Demonstration: Using the above-mentioned capabilities, VISK can generate hazard curves for centroid points of all the buildings identified within the case-study area as illustrated in Figures 8.

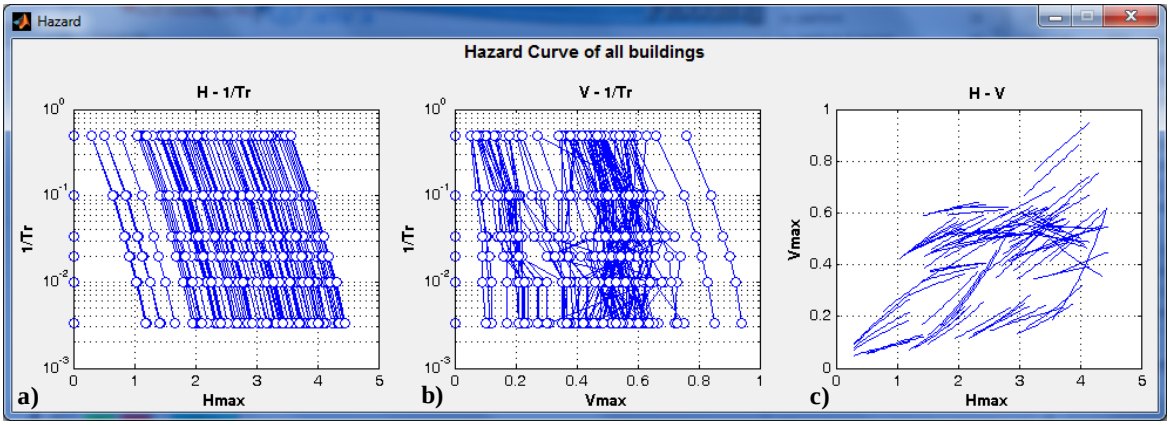

Figure 8: Hazard curves in terms of maximum flood a) height, b) velocity and c) relation between height and velocity, [17].

Figures 8a and 8b illustrate the hazard curves for all the building centroid points within a given case-study area for flooding height and velocity, respectively. For each building centroid, the set of $\mathbf{H}=[h_{max}, v_{max}]$ pairs and the power-law relation fitted to them are plotted in Figure 8c.

3 VISUAL VULNERABILITY ASSESSMENT PLATFORM

Structural vulnerability assessment lies in the core of VISK platform. The vulnerability assessment results are represented as the fragility curves, expressing the probability of exceeding a prescribed limit state. The software envisions various modes for acquiring the necessary input: (a) calculating the fragility curves based on the input provided to VISK; (b) creating Normal/Lognormal fragility curves based on the first two moments (i.e., mean and standard deviation); (c) creating fragility curves based on data uploaded by the user from a file; (d) creating step-function fragilities, referred to in the program as the Nominal fragilities. In this section the methodology used for calculating the fragility curves based on approach (a) listed above is described.

3.1 The limit states

The fragility curves are calculated for three limit states, namely, serviceability (SE), life safety (LS), and structural collapse (CO). In VISK, limit state thresholds are expressed in terms of the critical flooding height. Serviceability is marked by the critical water beyond which the normal activities in the household is going to be interrupted, most probably due to water infiltration. For example, for an insufficiently water-tight buildings built on a raised foundation, the critical serviceability water height is equal to the height of raised foundation above the ground level. For buildings constructed according to flood-resistant criteria, the critical water height for limit state of serviceability is taken asymptotically equal to the critical height needed for exceeding collapse limit state assuming brittle failure modes. Collapse limit state is defined as the critical flooding height in which the most vulnerable section of the most vulnerable wall in the building is going to break. Life safety limit state defines the critical flooding height in which lives of the inhabitants is going to be in danger. This can be caused either due to the infiltration of water inside the building (with the increasing risk of drowning in water), or the structural collapse (defined in the same manner as the critical height for collapse limit state). The critical water height for structural collapse is calculated in VISK by employing structural analysis taking into account the various sources of uncertainties in geometry, material properties and construction details. As far as it regards life safety considerations, VISK allows the consideration of judgment-based or code-based nominal water height.

For all the limit states considered within VISK, a simulation-based routine is employed in order to propagate the various sources of uncertainties described in Section 2.2. VISK employs an efficient simulation-based procedure relying on a small number of simulations (e.g., in the order of 50-100).

Assuming that vector $\boldsymbol{\theta}$ consists of all the uncertain parameters considered in the problem, simulation *i* corresponds to the i^{th} realization of vector $\boldsymbol{\theta}$. Each $\boldsymbol{\theta}_i$ is sufficient for defining the structural configuration, flood action, and material strength values for i^{th} simulation realization. Having this information, the critical water height can be calculated for each realization of the structural model/action. With reference to the uncertain parameters considered by VISK and described in Section 2.2, vector $\boldsymbol{\theta}$ is partitioned in two sections: $\boldsymbol{\theta}_1$ lists the discrete binary uncertain parameters considered; and $\boldsymbol{\theta}_2$ is related to continuous uncertain parameters. Each simulation realization is generated according to the probability distributions for vector $\boldsymbol{\theta}$ (at present, correlation structure is considered only for the discrete parameters defined using logic trees).

It is important to emphasize that the sampling procedure is going to involve both the structural model (configuration and material properties) and the flooding action. In particular, the load considered in the structural analysis is going to depend on the degree of water-tightness assigned to the structure based on the quality of doors and windows. Moreover, the parameters identifying the hydro-dynamic pressure profile have been simulated based on the variability of velocity profile with respect to the flooding height profile in the zone of interest, as demonstrated in detail in the section relative to the loading.

3.3 The structural analysis

VISK platform relies on the open-source structural finite element analysis software OpenSees [19] for structural analyses. The structural models developed herein are consisted of two-dimensional elastic shell finite element panels with openings (considered as voids). Three types of transversal boundary condition restraints are considered: (a) fixed end; (b) hinged; (c) free. For example, if a good transversal connection between two orthogonal walls is verified, wall panel with fixed-end restraints can be used. Based on the uncertain parame-

ters related to the geometrical configuration of the buildings, four different types of structural models are generated. These models are distinguished based on the type, number and relative positioning of openings (door and windows). Figure 9 below illustrates various configurations generated in the simulation procedure.

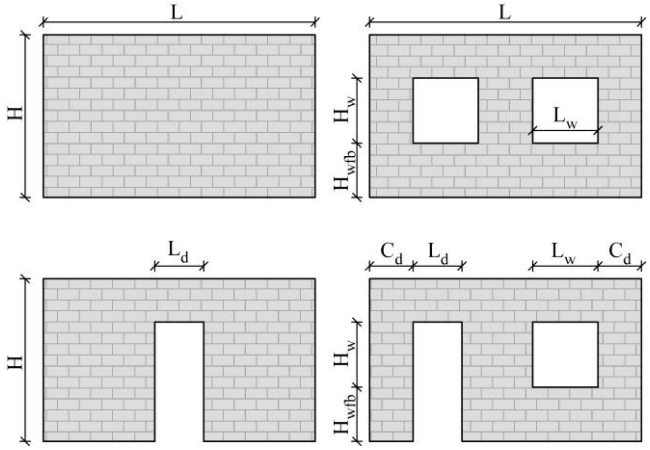

L (m) - wall length
H (m) - wall height
t (m) - wall thickness
L_w (m) - window length
H_w (m) - window height
H_{wfb} (m) - window rise
L_d (m) - door length
C_d (m) - corner length
H_f (m) - foundation rise
H_b (m) - barrier height

Figure 9: Four structural configurations considered in the analysis.

The current version of VISK considers three kinds of flood action on the structure: (1) hydrostatic; (2) hydrodynamic pressure; (3) waterborne debris impact; (4) material property deterioration (due to elongated contact with water). Detailed description of the above-mentioned flood actions can be found in [20]. As far as it regards the flooding pressure, the flooding profile across structural height is considered and the resulting forces are discretized to the panel joints. The discretized force on the openings (if they are sealed) is applied to the joints located at the opening boundary (neglected if the opening is not sealed).

3.3.1 Incremental flood loading analysis

The critical flooding height for the structure is established through a procedure referred to as incremental flood loading analysis. In this procedure, for increasing levels of flooding height, the structural model is analyzed considering the above-mentioned combination of actions (assuming that waterborne debris are going to hit the structure at the flooding water level assumed). The critical water-height for a given limits state is considered as the water-height in which the limit state in consideration is exceeded for the first time. For each flooding height level, this consists in controlling whether the section force, or demand, denoted by *D*, exceeds the corresponding section resistance, or capacity, denoted by *C*, for the specified limit state, for zones of stress concentration.

Safety-checking: For all the identified zones of stress concentration (described in detail in the next section) and for each water height level, safety-checking is performed in terms of both shear force and out-of-plane bending moment. It should be noted that safety-checking for bending moment is differentiated with respect to horizontal and vertical sections, due to the presence of axial forces. Denoting the flexural strength of a horizontal section by ($M_{Rd,H}$); the flexural strength of a vertical section by ($M_{Rd,V}$); and the shear strength by (V_{Rd}):

$$V_{Rd} = A_{section} \cdot \tau_0 \tag{3}$$

$$M_{Rd,H} = \frac{N \cdot t}{2} \cdot \left(1 - \frac{N}{0.85 \cdot f_m \cdot A_{section}}\right) \tag{4}$$

$$M_{Rd,V} = \frac{f_{fl} \cdot H_{section} \cdot t^2}{6} \tag{5}$$

where $A_{section}$ is the area of the section/sub-section; $H_{section}$ is the height of the section/sub-section, and N is the axial force acting on the section/sub-section. The formula for shear strength neglects interactions between shear/axial forces. The flexural strength for a horizontal section/sub-section in Eq. 4 is calculated assuming that the out-of-plane bending moment strength reached by exceeding the ultimate compression strength. This is while the flexural strength for a vertical section/sub-section in Eq.5 is calculated by assuming that the bending moment strength is reached by exceeding the ultimate tensile strength.

Calculating the critical demand-to-capacity ratio: VISK provides an iterative procedure for identification of the zones high stress concentration by searching through prescribed critical sections. Figure 10 below illustrates various critical sections (highlighted) identified in relation to structural configuration and geometry.

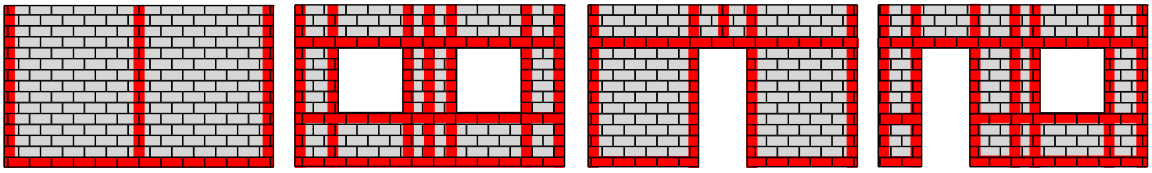

Figure 10: Zones of panel in which is searched the critical section.

Zones of high stress concentration can verify due to, debris impact, asymmetric boundary conditions, and geometrical configurations/presence of openings. Strictly speaking, local stress concentrations do not necessarily translate into global failure mechanisms; however, – in lieu of more accurate information – they can be considered as precursors to failure for a brittle structure. For each critical section *i* considered, the zone(s) of high stress concentration are identified by: (a) discretizing in smaller *sub-sections* (with a discretization step of 25 cm); (b) calculating the demand to capacity ratio (for both flexure and shear), for each sub-section *j* of the critical section considered, denoted by D_{ji}/C_{ji}. This is done in an exhaustive manner considering all the possible sub-sections; (c) defining the zone(s) of high stress concentration as those having the largest demand to capacity ratio $\max_j D_{ji}/C_{ji}$. In this manner, VISK can determine, for each water height level *h*, the critical demand to capacity ratio as the demand to capacity ratio *Y(h)* that takes the structure closer to the onset of specified limit state [21]:

$$Y(h) = \max_i \max_j \frac{Dji}{Cji} \tag{6}$$

VISK platform registers the critical section *i*, the mode of failure (shear/flexure), and the water height h_{cr} that corresponds to $Y(h_{cr})=1$.

For each Monte Carlo realization of the structural model identified by vector θ, a value for the critical water height $h_{cr}(\theta)$ is obtained, for a given limit state, defined as $Y(h_{cr}(\theta))=1$. The dependence of critical water-height on θ is dropped for convenience hereafter.

Numerical Example: Figure 11 below shows the histrogram of critical section/mode of failure corresponding to h_{cr} for a set of $N=200$ simulations performed by VISK. The red column marked as *no collapse* identifies the simulations in which, for all the water height levels considered, the critical height for which $Y(h_{cr})=1$ is not verified.

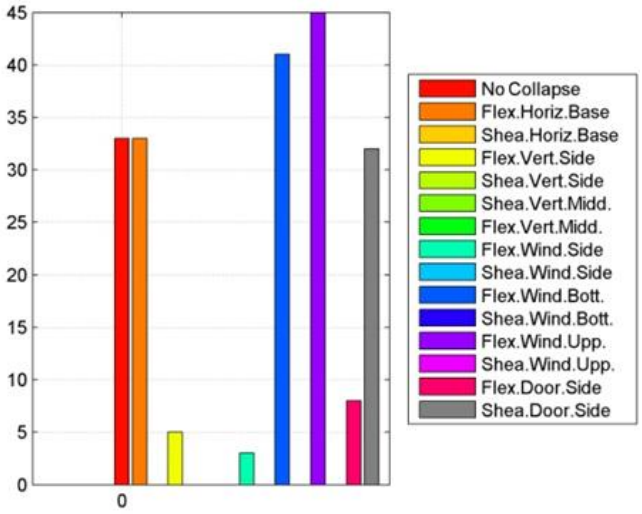

Figure 11. Histogram of critical section/mode of failure corresponding to h_{cr} for a set of $N=200$ simulations.

3.5 The analytical fragility curves

For each limit state considered, the simulation procedure provides a set of critical water height values as described in the previous section. These critical water height values are used then as *data* in order to calculate, using Bayesian parameter estimation [22], the *posterior* probability distribution for the parameters of prescribed analytic fragility functions. Finally, the *robust fragility* [23, 24] is calculated as the expected fragility based on the posterior probability distribution calculated for the parameters of the prescribed analytic fragility functions. Note that this posterior probability distribution can be interpreted as degrees of belief in the various analytic fragility models that are defined based on a specific set of parameters. VISK adopts three analytical fragility models corresponding to each of the three limit states considered:

(SE) $$F\left(h_f \mid \pi_0, \eta_{SE}, \beta_{SE}\right) = P\left(h_{SE} \le h_f\right) = \pi_0 \cdot \Phi\left(\frac{\ln \frac{h_f}{\eta_{SE}}}{\beta_{SE}}\right) + \left(1-\pi_0\right) \cdot I_0\left(h_f\right) \tag{7}$$

(CO) $$F\left(h_f \mid \eta_{CO}, \beta_{CO}\right) = P\left(h_{CO} \le h_f\right) = \Phi\left(\frac{\ln \frac{h_f}{\eta_{CO}}}{\beta_{CO}}\right) \tag{8}$$

(LS) $$F\left(h_f \mid \pi, \eta_{SL}, \beta_{SL}\right) = P\left(h_{SL} \le h_f\right) = \pi \cdot \Phi\left(\frac{\ln \frac{h_f}{\eta_{SL}}}{\beta_{SL}}\right) + \left(1-\pi\right) \cdot I\left(h_f\right) \tag{9}$$

where parameters π, η and β reported after the conditioning sign (|) are the three parameters that define the analytic probability distribution/fragility function for the serviceability (SE) and life safety (SL) limit states. Meanwhile, for the collapse (CO) limit state, only two parameters denoted by η and β are needed. 1-π_0 is the ratio of cases for which the serviceability critical height is equal to zero; *1-*π is the ratio of cases for which the life safety height is equal to a nominal prescribed value; η and β are respectively the median and the logarithmic standard deviation for the critical water height given that the critical water height is greater than zero for (SE) and given that the critical water height is not equal to the nominal value for (LS); Φ(.) denotes the standard Gaussian (Normal) cumulative probability distribution and $I_0(h_f)$ and $I(h_f)$ are index function defined as follows:

(SE)
$$I_0\left(h_f\right)=\begin{cases}0 \ if \ h_f=0\\ 1 \ if \ h_f>0\end{cases} \tag{10}$$

(LS)
$$I\left(h_f\right)=\begin{cases}0 \ if \ h_f\le h_{nominal}(LS)\\ 1 \ if \ h_f> h_{nominal}(LS)\end{cases} \tag{11}$$

$I_0(h_f)$ and $I(h_f)$ depict two step functions identified respectively by zero (Figure 12a) and the nominal water height ($h_{nominal}(LS)$) (Figure 12d). Note that the derivative *I* functions is equal to the Dirac delta function at $h=0$ and $h=h_{nominal}(LS)$.

The analytical fragility model proposed in Eq. 7 and Eq. 9 can be interpreted as an application of the total probability theorem [25] on the two mutually exclusive outcomes marked by probabilities π_0 and π. The probability distributions in Eqs. 7 and 9 are also known as the *three-parameter* distributions [25, 26] which are bi-modal probability density function (PDF)/cumulative distribution function (CDF) expressed as a linear combination of a Lognormal PDF/CDF and a Dirac delta function/step function. In particular, the three-parameter cumulative distribution functions expressed in Eq. 7 and illustrated in Figure 12(c) is a linear combination (with weight π_0) of the step function $I_0(h_f)$ depicted in Figure 12(a) and the Lognormal CDF depicted in Figure 12(b). In a similar manner, the three-parameter cumulative distribution functions expressed in Eq. 9 and illustrated in Figure 12(f) is a linear combination (with weight π) of the step function $I(h_f)$ depicted in Figure 12(d) and the Lognormal CDF depicted in Figure 12(e).

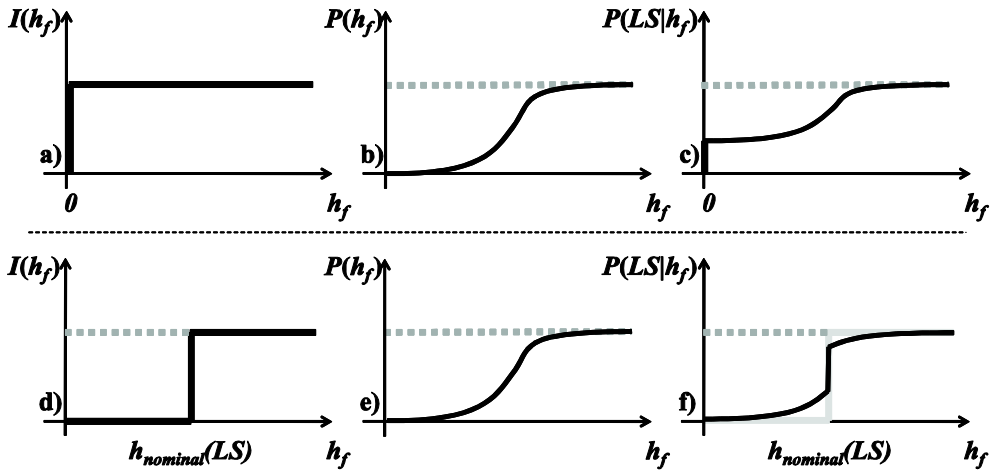

Figure 12: schematic diagrams of: a) step function for SE; b) the Lognormal CDF for SE; c) the three-parameter CDF for SE; d) step function for LS; e) the Lognormal CDF for LS; f) the three-parameter CDF for (LS)

3.6 The robust fragility estimation

Denoting the parameters of the analytic fragility function as χ (e.g., $\chi=[\pi,\eta,\beta]$ for LS), the joint probability distribution for the vector of parameters χ can be expressed as $p(\chi)$. Using Bayesian parameter estimation, the probability distribution for the parameters of the fragility function for a given limit state can be updated using formulas described in [22] based on the set of critical height values obtained from simulation. The updated or posterior probability distribution can be denoted as $p(\chi|\mathbf{H_c(LS)})$ [3] where $\mathbf{H_c(LS)}$ is the vector of simulation-based critical height values for limit state LS. This probability distribution represents the uncertainty in the vector χ due to limited number of simulations.

The robust fragility denoted by $F(h_f|\ \mathbf{H_c})$ is calculated as the expected value of the analytic function $F(h_f|\chi)$ in Eqs. 3, 4 and 5, over the entire domain of vector χ and according to the updated joint probability distribution $p(\chi|\mathbf{H_c})$:

$$F\left(h_f \mid \boldsymbol{H_c}\right) = E\left[F\left(h_f \mid \chi\right)\right] = \int_{\Omega} F\left(h_f \mid \chi\right) \cdot p\left(\chi \mid \boldsymbol{H}_c\right) \cdot d\chi \tag{12}$$

where $E[.]$ is the expected value operator and Ω is the domain of the vector χ. The variance σ^2 in fragility estimation can be calculated as:

$$\sigma^2\left[F\left(h_f \mid \chi\right)\right] = E\left[F\left(h_f \mid \chi\right)^2\right] - E\left[F\left(h_f \mid \chi\right)\right]^2 \tag{13}$$

where $E[F(h_f|\chi)]^2$ can be calculated from Eq. 12 replacing $F(h_f|\chi)$ with $F(h_f|\chi)^2$.

Numerical Example: Figure 13 below illustrates the robust fragility curves and their plus/minus one standard deviation interval, corresponding to the three limit states (SE, LS and CO) taken into account into in VISK, based on N=50 Monte Carlo simulations.

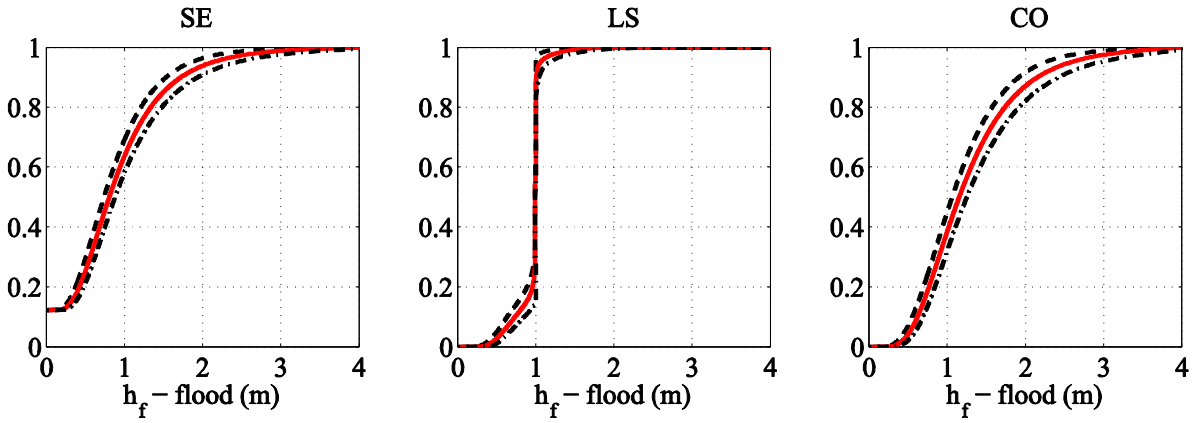

Figure 13: Robust Fragility curves and their plus/minus one standard deviation interval (SE), (LS) and (CO), respectively.

[3] LS is dropped hereafter for brevity.

4 VISUAL RISK ASSESSMENT PLATFORM

4.1 The risk maps

VISK renders point estimates of flooding risk by integrating the robust fragility and its plus/minus one standard deviation intervals ($F \pm \sigma_F$) and the flood hazard at a given point in the zone of study:

$$\lambda_{LS}(\mathbf{H_c}) = \int_x \mathrm{F}\left(x \mid \mathbf{H_c}\right) \cdot \left| d\lambda\left(x\right) \right| \cdot dx \tag{14}$$

In this case, the flooding risk is $\lambda_{LS}(\mathbf{H_c})$ is expressed in terms of the mean annual rate of exceeding[4] a prescribed limit state LS (i.e., exceeding the critical flooding height corresponding to the limit state in question) for a given point. The annual probability of exceeding a limit state *P(LS)*, assuming a homogeneous Poisson process model with rate λ_{LS} is:

$$P\left(LS\right) = 1 - \exp\left(-\lambda_{LS}\right) \tag{15}$$

Numerical Example: Figure 14 illustrates risk maps in terms of mean annual rate λ_{LS} and annual probability *P(LS)* of exceeding the collapse limit state.

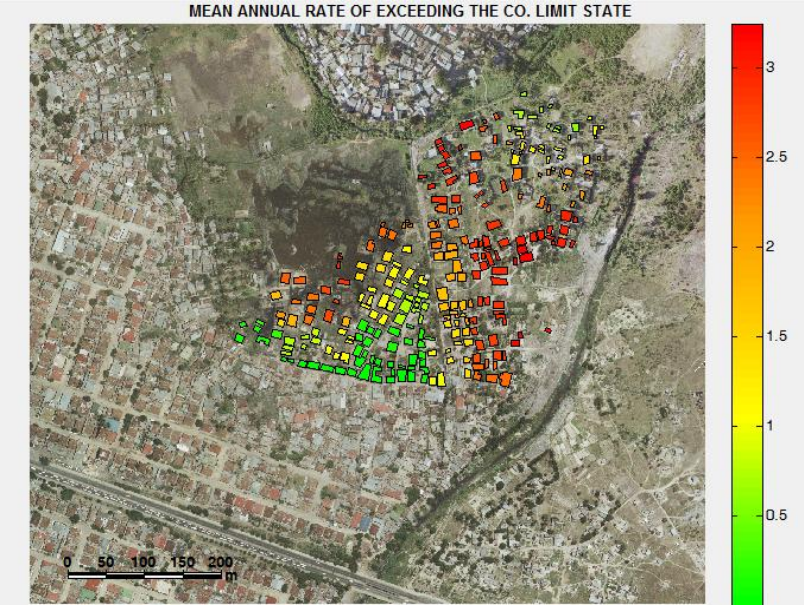

Figure 14 a: Risk maps in terms of mean annual rate of exceeding the collapse limit state [17]

[4] $\mathbf{H_c}$ is dropped hereafter for brevity.

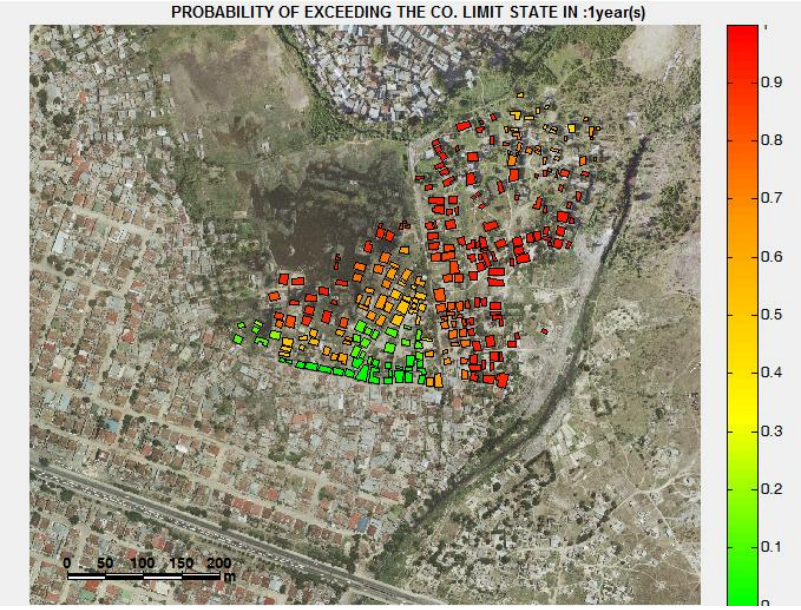

Figure 14 b: Risk maps in terms of the annual probability of exceeding the collapse limit state [17]

Exposure to risk: VISK estimates the exposure to risk by calculating the total expected loss or the expected number of people affected for all the buildings identified (see Section 2.1) in the case-study area. The expected repair cost (per building or per unit residential area), E[R], can be calculated as a function of the limit state probabilities and by defining the damage state *i* as the structural state between limit states *i* and *i*+1:

$$E[R] = \sum_{i=1}^{N_{LS}} \left[P\left(LS_{i+1}\right) - P\left(LS_i\right) \right] \cdot R_i \tag{16}$$

where N_{LS} is the number limit states that are used in the problem in order to discretize the structural damage; R_i is the repair cost corresponding to damage state *i*; and $P\left(LS_{N_{LS}+1}\right) = 0$.

The expected number of people affected by flooding can also be estimated as a function of the limit state probabilities from Eq. (16) replacing R_i by the population density (per house or per unit residential area).

Numerical Example: Considering a population density of 0.03 per residential square meter and a rebuilding cost of 3 € per square meter (for a single limit state, CO), the expected replacement cost and the expected number of casualties is calculated from Eq. 16 (with $N_{LS}=1$). Figure 15 and 16 illustrate the expected number of casualties and expected replacement cost for the buildings considered in the case-study area.

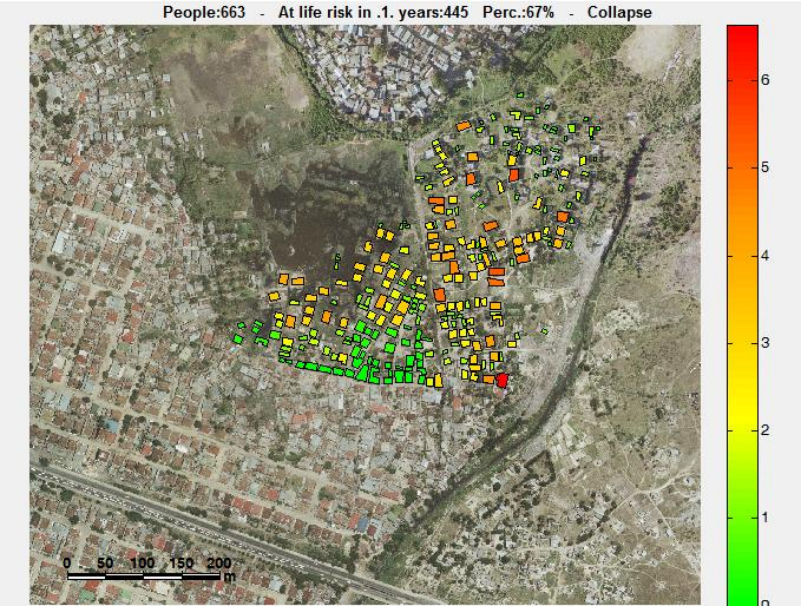

Figure 15: The expected number of casualties [17]

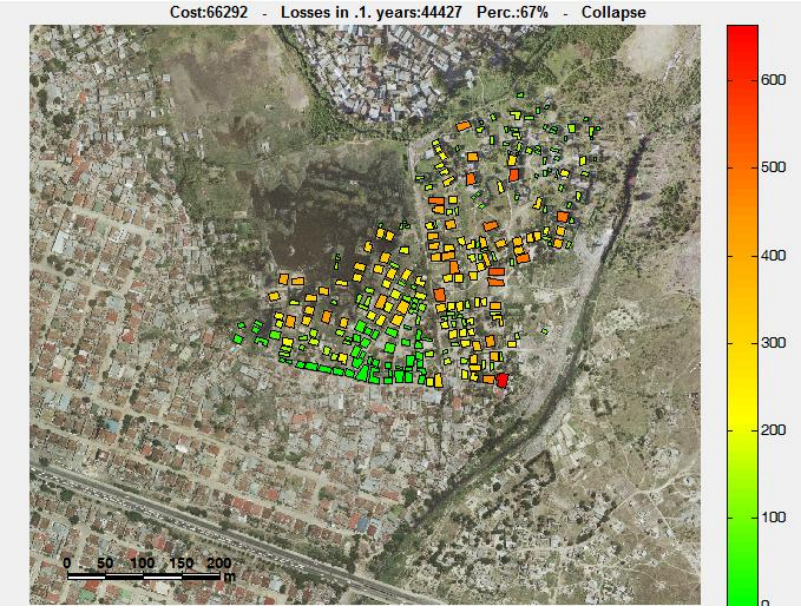

Figure 16: The expected replacement cost [17]

2 CONCLUSION

VISK is a new software platform with a graphical user interface for micro-scale flood risk assessment for a single class of buildings. This software, which has been developed in the context of the European FP7 project CLUVA for flood vulnerability assessment of informal settlements ("non-engineered" buildings), is particularly suitable for risk assessment based on incomplete information. This paper has discussed the novel features of VISK. These novel features include: using manual orthophoto boundary recognition in order to capture the footprint of the buildings considered; propagation of several sources of uncertainties (e.g., building-to-building variability, incomplete knowledge, limited number of surveys, limited number of simulations) in the calculation of structural fragility for a class of buildings; considering the correlation between discrete binary parameters; using Bayesian parameter estimation based on sample field survey results in order to characterize uncertainties; calculating the structural

fragility using an efficient Bayesian small-sample simulation method; an exhaustive iterative procedure for localizing the structural damage in the model structure; considering the openings in the model structure; taking into account flood actions such as the hydro-static and hydro-dynamic pressure, the debris impact and material deterioration due to elongated contact with water, taking into account the effect of water-seepage in structural analysis. The fragility curves for the class of buildings are calculated for three limit states of serviceability (SE), structural collapse (CO), and life safety (LS). Various point-wise risk metrics are adopted in VISK for evaluating the flooding risk, the mean annual rate and annual probability of exceeding a prescribed limit state, the expected loss, and the expected number of people affected by flooding.

It should be noted that, although VISK is developed for micro-scale flood risk assessment of informal settlements, it could be applied to other building types in general.

ACKNOWLEDGEMENTS AND DATA SOURCES

This work was supported in part by the European Commission's seventh framework program Climate Change and Urban Vulnerability in Africa (CLUVA), FP7-ENV-2010, Grant No. 265137. This support is gratefully acknowledged. The authors gratefully acknowledge Prof. F. De Paola, Prof. M. Giugni and M. E. Topa for providing the inundation profiles; E. Mbuya and A. Kyessi for the field survey results for informal settlements in Suna Sub-ward of Dar es Salaam City.

REFERENCES

[1] Jonkman S.N., Vrijling J.K., and Vrouwenvelder A.C.W.M., *Methods for the estimation of loss of life due to floods: a literature review and a proposal for a new method.* Natural Hazards, 2008. **46**: p. 353-389.

[2] Pistrika A.K. and Jonkman S.N., *Damage to residential buildings due to flooding of New Orleans after hurricane Katrina.* Natural Hazards, 2009. **54**: p. 413-434.

[3] Pistrika A. and Tsakiris G., *Flood risk assessment: A methodological framework*, in *Water Resources Management: New Approaches and Technologies. European Water Resources Association, Chania, Crete-Greece*. 2007.

[4] Pistrika A., *Flood Damage Estimation based on Flood Simulation Scenarios and a GIS Platform*, in *EWRA 7th International Conference "Water Resources Conservancy and Risk Reduction Under Climatic Instability"*. 2009: Limassol, Cyprus. p. 419-427.

[5] Smith D., *Flood damage estimation- A review of urban stage-damage curves and loss functions.* Water S. A., 1994. **20**(3): p. 231-238.

[6] Kang J., Su M., and Chang L., *Loss functions and framework for regional flood damage estimation in residential area.* Journal of Marine Science and Technology, 2005. **13**(3): p. 193-199.

[7] Schwarz J. and Maiwald H., *Empirical vulnerability assessment and damage for description natural hazards following the principles of modern macroseismic scales*, in *14th WCEE - World Conference of Earthquake Engineering*. 2012: Lisboa, Portugal.

[8] Schwarz J. and Maiwald H., *Damage and loss prediction model based on the vulnerability of building types*, in *4th International symposium of Flood Defence*. 2008: Toronto, Canada.

[9] Nadal N.C., Zapata R.E., Pagán I., López R., and Agudelo J., *Building damage due to riverine and coastal floods.* Journal of Water Resources Planning and Management, 2009. **136**(3): p. 327-336.

[10] Scawthorn C., Flores P., Blais N., Seligson H., Tate E., Chang S., Mifflin E., Thomas W., Murphy J., and Jones C., *HAZUS-MH flood loss estimation methodology. II. Damage and loss assessment.* Natural Hazards Review, 2006. **7**(2): p. 72-81.

[11] Scawthorn C., Blais N., Seligson H., Tate E., Mifflin E., Thomas W., Murphy J., and Jones C., *HAZUS-MH flood loss estimation methodology. I: Overview and flood hazard characterization.* Natural Hazards Review, 2006. **7**(2): p. 60-71.

[12] Apel H., Aronica G.T., Kreibich H., and Thieken A.H., *Flood risk analyses—how detailed do we need to be?* Natural Hazards, 2008. **49**: p. 79-98.

[13] Faber M.H., *Statistics and Probability Theory: In Pursuit of Engineering Decision Support*. Vol. 18. 2012: Springer.

[14] Jaynes E.T., *Probability theory: The logic of science*. 2003: Cambridge university press.

[15] O'Brien J., Julien P., and Fullerton W., *Two-dimensional water flood and mudflow simulation.* Journal of hydraulic engineering, 1993. **119**(2): p. 244-261.

[16] FLO-2D S.I., *FLO-2D® User's Manual*. 2004: Nutrioso, Arizona.

[17] DeRisi R., Jalayer F., DePaola F., Iervolino I., Giugni M., Topa M.E., Mbuya E., Kyessi A., Manfredi G., and Gasparini P., *Flood Risk Assessment for Informal Settlements, Under Review.* Natural Hazards, 2013.

[18] DeRisi R., Jalayer F., Iervolino I., Kyessi A., Mbuya E., Yeshitela K., and Yonas N., *Guidelines for vulnerability assessment and reinforcement measures of adobe houses*, deliverable in CLUVA project - Climate Change and Urban Vulnerability in Africa. 2012. Available from: http://www.cluva.eu/deliverables/CLUVA_D2.4.pdf. Data last access: 01/01/2013.

[19] McKenna F., Fenves G., and Scott M., *OpenSees: Open system for earthquake engineering simulation.* Pacific Earthquake Engineering Center, University of California, Berkeley, CA., http://opensees. berkeley. edu, 2006.

[20] Kelman I. and Spence R., *An overview of flood actions on buildings.* Engineering Geology, 2004. **73**(3): p. 297-309.

[21] Jalayer F., Franchin P., and Pinto P., *A scalar damage measure for seismic reliability analysis of RC frames.* Earthquake Engineering & Structural Dynamics, 2007. **36**(13): p. 2059-2079.

[22] Box G.E.P. and Tiao G.C., *Bayesian Inference in Statistical Analysis*, ed. W. Interscience. 1992: John Wiley & Sons, Inc.

[23] Jalayer F., Elefante L., Iervolino I., and Manfredi G., *Knowledge-based performance assessment of existing RC buildings.* Journal of Earthquake Engineering, 2011. **15**(3): p. 362-389.

[24] Papadimitriou C., Beck J.L., and Katafygiotis L.S., *Updating robust reliability using structural test data.* Probabilistic Engineering Mechanics, 2001. **16**(2): p. 103-113.

[25] Benjamin J.R. and Cornell C.A., *Probability, Statistics, and Decision for Civil Engineers*. 1970: McGraw-Hill, New York.

[26] Shome N., *Probabilistic seismic demand analysis of nonlinear structures*. RMS Program. 1999, Stanford University.